Pressure Support Ventilation and Biphasic Positive Airway Pressure Improve Oxygenation by Redistribution of Pulmonary Blood Flow

Alysson R. Carvalho, PhD*†

Peter M. Spieth, MD*

Paolo Pelosi, MD, PhD‡

Alessandro Beda, PhD*

Agnaldo J. Lopes, MD, DSc†

Boriana Neykova, MD§

Axel R. Heller, MD, PhD*

Thea Koch, MD, PhD*

Marcelo Gama de Abreu, MD, MSc, PhD, DEAA*

BACKGROUND: Spontaneous breathing (SB) activity may improve gas exchange during mechanical ventilation mainly by the recruitment of previously collapsed regions. Pressure support ventilation (PSV) and biphasic positive airway pressure (BIPAP) are frequently used modes of SB, but little is known about the mechanisms of improvement of lung function during these modes of assisted mechanical ventilation. We evaluated the mechanisms behind the improvement of gas exchange with PSV and BIPAP.

METHODS: Five pigs (25–29.3 kg) were mechanically ventilated in supine position, and acute lung injury (ALI) was induced by surfactant depletion. After stabilization, BIPAP was initiated with lower continuous positive airway pressure equal to 5 cm H_2O and the higher continuous positive airway pressure titrated to achieve a tidal volume between 6 and 8 mL/kg. The depth of anesthesia was reduced, and when SB represented ≥20% of total minute ventilation, PSV and BIPAP + SB were each performed for 1 h (random sequence). Whole chest helical computed tomography was performed during end-expiratory pauses and functional variables were obtained. Pulmonary blood flow (PBF) was marked with IV administered fluorescent microspheres, and spatial cluster analysis was used to determine the effects of each ventilatory mode on the distribution of PBF.

RESULTS: ALI led to impairment of lung function and increase of poorly and nonaerated areas in dependent lung regions ($P < 0.05$). PSV and BIPAP + SB similarly improved oxygenation and reduced venous admixture compared with controlled mechanical ventilation ($P < 0.05$). Despite that, a significant increase of nonaerated areas in dependent regions with a concomitant decrease of normally aerated areas was observed during SB. In five of six lung clusters, redistribution of PBF from dependent to nondependent, better aerated lung regions were observed during PSV and BIPAP + SB.

CONCLUSIONS: In this model of ALI, the improvements of oxygenation and venous admixture obtained during assisted mechanical ventilation with PSV and BIPAP + SB were explained by the redistribution of PBF toward nondependent lung regions rather than recruitment of dependent zones.

Controlled mechanical ventilation may be necessary to achieve adequate gas exchange and reduce the work of breathing in patients with acute lung injury (ALI).[1–3] However, clinical and experimental studies have shown that spontaneous breathing (SB) activity may improve gas exchange and lung function during mechanical ventilation, as well as reduce the need for sedation, cardio-circulatory drug support,[4–6] and even mitigate atrophy of diaphragm myofibers.[7]

Controlled mechanical ventilation with deep sedation and/or muscle paralysis also modifies the displacement pattern of the diaphragm.[8,9] The unopposed increase of intraabdominal pressure may reduce the transpulmonary pressure in dependent lung regions, promoting lung collapse[5,8] and redistributing tidal ventilation toward nondependent regions.[10,11] In this context, SB activity may contribute to restoring the physiological displacement of the diaphragm, improving regional ventilation of dependent lung regions[12] and enhancing hemodynamics through decreased intrathoracic pressure.[2,13–15] The recruitment of dorsal and usually better perfused lung regions through inspiratory efforts is considered the main mechanism behind the improvement in gas exchange during

From the *Clinic of Anesthesiology and Intensive Care Medicine, University Clinic Carl Gustav Carus, Dresden, Germany; †University Augusto Motta, Rio de Janeiro, Brazil; ‡Department of Ambient, Health and Safety, University of Insubria, Varese, Italy; and §Institute of Radiology, University Clinic Carl Gustav Carus, Technical University Dresden, Dresden, Germany.

Accepted for publication May 4, 2009.

Supported, in part, by a research grant from the European Society of Anaesthesiology, Brussels, Belgium.

Address for correspondence and reprint requests to Dr. Marcelo Gama de Abreu, Clinic of Anesthesiology and Intensive Care Medicine, University Clinic Carl Gustav Carus, Technical University Dresden, Fetscherstr. 74, 01307 Dresden, Germany. Address e-mail to mgabreu@uniklinikum-dresden.de.

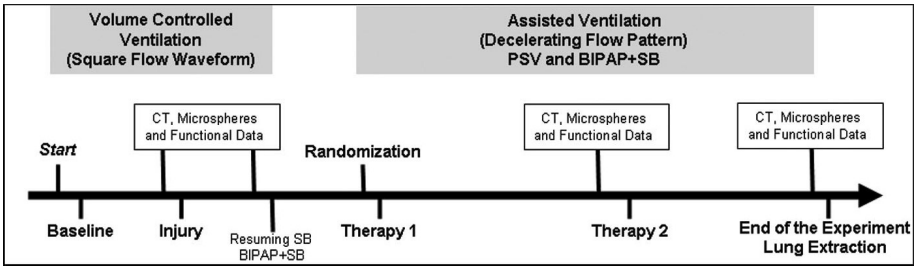

Figure 1. Time course of interventions. Therapy 1 and 2 correspond to the sequence of spontaneous breathing (pressure support ventilation [PSV] or biphasic positive airway pressure [BIPAP] + spontaneous breathing [SB]) after the randomization.

assisted ventilation,[5,8,12] but this concept was challenged recently.[16]

Pressure support ventilation (PSV) and biphasic positive airway pressure with SB (BIPAP + SB), both characterized by decelerating inspiratory flow patterns, are frequently used modes of mechanical ventilation in the clinical arena. Although PSV supports every triggered breath with positive pressure, BIPAP allows SB without support at two different airway pressure levels. This may lead to enhanced ventilation and perfusion of dependent lung regions, making BIPAP + SB superior to PSV.[3,17] However, more recent works have suggested that PSV and BIPAP + SB similarly improve gas exchange when compared with controlled mechanical ventilation in experimental ALI.[16,18]

The main objective of this study was to identify the mechanisms behind the improvement in lung function during PSV and BIPAP + SB. For this purpose, we assessed the distribution of lung aeration and the spatial distribution of changes in pulmonary perfusion, so-called clusters, during PSV and BIPAP + SB in experimental ALI. We hypothesized that redistribution of pulmonary blood flow (PBF) toward better aerated regions plays an important role in the improvement of oxygenation during PSV and BIPAP + SB.

METHODS

Experimental Protocol

The protocol of this study was approved by the local animal care committee and the Government of the State of Saxony, Germany. Figure 1 shows the sequence of interventions performed, which are described in detail in this section. Five female pigs were anesthetized and mechanically ventilated with volume-controlled mode with inspiratory square flow waveform using a tidal volume (V_T) = 12 mL/kg, I:E = 1:1, inspired oxygen fraction (FIO_2) = 0.5, positive end-expiratory pressure = 5 cm H_2O, and respiratory rate (RR) set to achieve an arterial pressure of carbon dioxide ($PaCO_2$) between 30 and 45 mm Hg.

Measurements of Functional Variables

Airway (Paw) and esophageal (Pes) pressures as well as airflow ($\dot{V}$) were continuously recorded.[19] The product of Pes versus time (PTP) was calculated during inspiration, taking the first value at the beginning of the inspiratory cycle as offset. Respiratory drive ($P_{0.1}$) was assessed as the difference between Paw at the beginning of inspiration and 100 ms thereafter.[16] Mean systemic and pulmonary arterial pressures as well as central venous and pulmonary artery wedge pressures were measured. Cardiac output, venous admixture, and oxygen delivered and consumption were calculated using standard formulas.[20]

Computed Tomography

Helical computed tomography (CT) scans of the whole lung were obtained with a Somatom Sensation 16 (Siemens, Erlangen, Germany) during controlled mechanical ventilation, before and after the induction of ALI, as well as during assisted mechanical ventilation with PSV and BIPAP + SB. Scans were obtained during breath-hold maneuvers at end-expiratory pressure and with simultaneous clamping of the endotracheal tube. The CT scanner was set as follows: collimation, 16 × 0.75 mm; pitch, 1.35; bed speed, 38.6 mm/s; voltage, 120 kV; and tube current-time product, 120 mAs. Images were reconstructed with slices of 5 mm thickness, without gaps between slices, yielding images with 512 × 512 pixels with a surface of 0.443 × 0.443 mm^2 (voxel size = 0.98 mm^3).

The radiograph attenuation of each pixel, expressed in Hounsfield units (HU), was primarily determined by the density (mass/volume ratio) of the tissue and expressed as the CT number, i.e., CT/(−1000) = (volume of gas/[volume of gas + volume of tissue]). The attenuation scale arbitrarily assigns to bone a value of 1000 HU (complete absorption), to air a value of −1000 HU (no absorption), and to water a value of 0 HU; blood and lung tissue have a density ranging between 20 and 40 HU.[21,22] After manual segmentation of the region of interest, images were analyzed for calculation of total lung and total gas volumes as well as total lung mass and percentages of hyperaerated (−1000 to −900 HU), normally aerated (−900 to −500 HU), poorly aerated (−500 to −100 HU), and nonaerated (−100 to +100 HU) compartments in total lung volume, as suggested elsewhere.[21,22]

The lung volume (i.e., the sum of gas plus tissue volume) was calculated as follows: ([size of the pixel]^2 × slice thickness × total number of pixels of the region of interest for the whole lung). Weight of

lungs was calculated as: ([1 − CT/−1000] × [size of the pixel]^2 × slice thickness × total number of pixels of the region of interest for the whole lung).[22]

To assess the regional distribution of aeration in noninjured and injured lungs as well as in controlled and assisted ventilation, the whole lung was divided into 10 zones in the cranio-caudal and also the ventro-dorsal axes. The median CT-scan attenuation and the volume of each zone were calculated.

Three-dimensional volume meshes were created by masking the lung boundary of each compartment with a routine written in Matlab (MathWorks) by one of the authors (ARC). Color mapping was used to represent lung aeration compartments.

Distribution of PBF

Regional PBF was marked with IV administered fluorescent, color-labeled 15-μm diameter microspheres before and after induction of lung injury in controlled mechanical ventilation as well as during assisted mechanical ventilation with PSV and BIPAP + SB. The colors used were blue-green, carmine, crimson, red, orange, scarlet, and yellow-green. A different color was assigned randomly and administered at each timepoint to mark regional perfusion under each experimental condition. Immediately before injection, the microspheres were vortexed, sonicated for 90 s, and drawn into a 2-mL syringe. All injections were performed over 60 s to average blood flow over several cardiac cycles and V_Ts. During injection, approximately 1.5 × 10^6 microspheres were administered.

Postmortem processing of lungs was performed as previously described.[23] Briefly, lungs were flushed with 50 mL/kg of a hydroxyethyl starch 130/0.4 solution (Voluven, Fresenius Kabi, Bad Homburg, Germany) and air-dried by continuous tracheal airflow for 7 days (continuous pressure of 25 cm H_2O). The lungs were then coated with a one-component polyurethane foam (BTI Befestigungstechnik, Ingelfingen, Germany), suspended vertically in a square box, and embedded in rapidly setting urethane foam (polyol and isocyanate, Elastogran, Lemförde, Germany). The foam block was cut into cubes of 1.3 cm^3. Each cube was weighed and assigned a three-dimensional coordinate. The samples were then soaked for 2 days in 2 mL of 2-ethoxyethyl acetate (Aldrich Chemical, Milwaukee, WI) to retrieve the fluorescent dye. The fluorescence was read in a luminescence spectrophotometer (LS-50B; Perkin-Elmer, Beaconsfield, UK). The measured intensity of fluorescence in each probe was normalized according to its own weight using Eq. 1:

$$\dot{Q}_{rel,i} = x_i/(\sum x_i)/n \quad (1)$$

where $\dot{Q}_{rel,i}$ is the weight-normalized relative PBF of the probe i; x_i is the obtained fluorescence divided by the weight of the probe i, and n is the number of probes. The mean normalized relative flow was therefore 1.0.

The distribution of PBF along the cranio-caudal and ventro-dorsal axes under each experimental condition was assessed by means of linear regression. Additionally, a three-dimensional reconstruction of the lung was performed, considering the spatial coordinates of each lung piece and the PBF at each of the x, y, and z coordinates. Color mapping was used to identify the regional distribution of PBF based on $\dot{Q}_{rel,i}$. The color map was then normalized by the maximum $\dot{Q}_{rel}$ under each experimental condition, resulting in a color scale ranging from dark blue (0.0, lowest perfusion) to dark red (1.0, highest perfusion). Thereafter, the lungs were divided into 10 zones of equal heights along the cranio-caudal and ventro-dorsal axes, as described, for CT analysis. The relative blood flow content ($\dot{Q}_{rel}$ content) of each zone was calculated taking the sum of $\dot{Q}_{rel,i}$ in that zone divided by the sum of $\dot{Q}_{rel}$ in the whole lung. The volume of each zone was also computed by the simple arithmetical sum of each lung piece in that zone.

The spatial representation of the lung volume meshes and the distribution of PBF were obtained using a routine written in Matlab (MathWorks) by one of the authors (ARC).

Experimental Protocol

After instrumentation, animals were allowed to stabilize for 15 min (baseline). ALI was induced by repetitive lung lavage until the Pao_2/Fio_2 ratio decreased to <200 mm Hg and did not spontaneously recover during a 30-min period.[24] The endotracheal tube was disconnected from the ventilator and warmed isotonic saline solution (30 mL/kg, 37°C–39°C) was instilled (height of approximately 40 cm above the endotracheal tube). After that, the fluid was retrieved passively by gravity drainage. Further lavages were performed if Pao_2/Fio_2 ratio exceeded 200 mm Hg. The countdown of 30 min was restarted in this case. After injury stabilization, the ventilator was switched to BIPAP with lower continuous positive airway pressure ($CPAP_{low}$) = 5 cm H_2O, higher CPAP ($CPAP_{high}$) titrated to obtain V_T between 6 and 8 mL/kg, and RR to achieve $Paco_2$ between 50 and 60 mm Hg without SB. The depth of anesthesia was reduced (0.5–1.5 $mg \cdot kg^{-1} \cdot h^{-1}$, midazolam; 4–6 $mg \cdot kg^{-1} \cdot h^{-1}$, ketamine; and 0.1–0.3 $\mu g \cdot kg^{-1} \cdot h^{-1}$, remifentanil), and when SB represented more than 20% of total minute ventilation, the ventilatory mode was switched to PSV or BIPAP + SB. During PSV, pressure support was set to obtain V_T between 6 and 8 mL/kg, the flow trigger was 2.0 L/min, and the cycling-off criteria was 25% of peak flow. During BIPAP + SB, the I:E ratio was adjusted to obtain mean Paw in the range of 8–10 cm H_2O to permit comparability with the PSV mode. The animals' lungs were then ventilated for a period of 1 h with each mode (random sequence).

Table 1. Respiratory Variables

	Controlled ventilation (square inspiratory flow pattern)		Assisted ventilation (decelerating inspiratory flow pattern)	
	Baseline	Injury	PSV	BIPAP + SB
MV				
Total (L/min)	4.5 (3.3–6.8)	3.6 (3.3–4.6)	6.8† (5.8–7.1)	7.1† (4.9–7.3)
Controlled (L/min)	4.5 (3.3–6.8)	3.6 (3.3–4.6)	—	1.5† (1.3–1.6)
Spontaneous (L/min)	—	—	—	5.3 (3.6–5.6)
V_T				
Total (mL)	324.7 (320.7–333.4)	332.0 (313.5–333.2)	160.1† (130.4–165.1)	109.9†‡ (91.0–113.4)
Controlled (mL)	324.7 (320.7–333.4)	332.0 (313.5–333.2)	—	157.8 (141.4–169.2)
Spontaneous (mL)	—	—	—	93.2 (86.5–109.4)
RR				
Total (/min)	14(10–20)	12 (10–13)	35† (31–52)	55† (49–66)
Controlled (/min)	14 (10–20)	12 (10–13)	—	10 (6–12)
Spontaneous (/min)	—	—	—	45 (39–60)
Ppeak				
Total (cm H_2O)	18.9 (18.8–19.2)	31.7* (30.1–32.6)	22.1† (21.8–22.5)	10.5† (9.8–11.6)
Controlled (cm H_2O)	18.9 (18.8–19.2)	31.7* (30.1–32.6)	—	22.3† (22.0–22.5)
Paw mean (cm H_2O)	10.7 (10.5–10.8)	14.9* (13.3–15.3)	7.8† (7.6–8.9)	9.4†‡ (9.1–9.8)
$P_{0.1}$ (cm H_2O)	—	—	0.43 (0.4–0.6)	4.9‡ (2.2–5.2)
PTP (cm $H_2O \cdot s \cdot min^{-1}$)	—	—	30.8 (15.3–39.7)	168.6‡ (106.4–192.2)

Values provided as median (interquartile ranges).

PSV = pressure support ventilation; BIPAP + SB = biphasic positive airway pressure + spontaneous breathing; MV = minute ventilation; V_T = tidal volume; RR = respiratory rate; Ppeak = peak airway pressure; Paw mean = mean airway pressure; $P_{0.1}$ = airway pressure gradient measured at 100 ms after start of inspiration; PTP = inspiratory pressure time product of esophageal pressure; –, not applicable.

* $P < 0.05$ versus baseline; † $P < 0.05$ versus injury; ‡ $P < 0.05$ versus PSV.

CT-scan images, fluorescent microspheres injection, and functional variables measurements were performed under each experimental condition (Fig. 1). Animals were then killed by IV administration of 2 g of thiopental and 50 mL of KCl (1 M), and lungs were extracted for determination of PBF distribution.

Postmortem Lung Processing

Lungs were air-dried at 25 cm H_2O for 7 days and cut into pieces of approximately 1.33 mm^3. The intensity of fluorescence in each piece was measured and normalized for its own weight.[23] A three-dimensional reconstruction of the lung was performed, considering the spatial coordinates of each lung piece and the PBF at each of the x, y, and z coordinates. Thereafter, lungs were divided into 10 zones along the cranio-caudal and ventro-dorsal axes and the relative blood flow content of each zone was calculated.

Cluster Analysis

For each animal, lung pieces sharing similar characteristics of change in PBF were grouped into clusters. In addition, meta-cluster analysis was used to identify stereotypical changes in PBF that were common to all animals.[25] For this purpose, the pieces from all animals were merged into one dataset and the nonhierarchical clustering method was used to identify clusters that have the same pattern across all animals. Accordingly, clustering of pieces from individual animals shows whether changes in flow over each experimental condition occur in different parts of the lung, and the meta-clustering demonstrates whether the pattern of change is common across animals.

To verify if a single dominant animal influenced the clustering processing in the meta-cluster, the amount of each animal's pieces in each respective cluster was calculated. Because five animals were studied, we expected that the ideal cluster from the meta-cluster procedure should be composed of a fraction of 20% of pieces per animal. However, values between 20% ± 10% were accepted.

The clusters were created without reference to the spatial location of pieces within the lung. To display and assess spatial clustering using data from meta-clusters, a "meta-lung" was created by linear transformations (stretching and compressing) along the x, y, and z axes of the coordinates for each animal, as previously proposed.[25]

Statistical Analysis

Values are presented as median and interquartiles (1st quartile–3rd quartile). Comparisons were performed using Wilcoxon's test for paired data (Software package SPSS, version 12.0, Chicago, IL), and the Bonferroni-Holm procedure was used to adjust for multiple tests. Statistical significance was set at $P < 0.05$.

RESULTS

Surfactant depletion increased Paw (Table 1), impaired oxygenation, and worsened venous admixture (Table 2). Furthermore, increases in total lung volume,

Table 2. Gas Exchange, Hemodynamics, and Oxygen Transport/Consumption

	Controlled ventilation (square flow waveform)		Assisted ventilation (decelerating flow pattern)	
	Baseline	Injury	PSV	BIPAP + SB
Gas exchange				
Pao_2/Fio_2 (mm Hg)	533.2 (517.6–536.8)	126.0* (102.0–141.4)	262.8† (243.2–290.4)	218.8† (198.2–229.4)
$\dot{Q}_{VA}/\dot{Q}_t$ (%)	5.5 (5.1–6.9)	26.1* (25.2–33.1)	16.7† (9.8–17.4)	19.2† (13.5–19.7)
$Paco_2$ (mm Hg)	33.1 (30.9–36.7)	37.2 (35.4–37.8)	55.0† (49.6–55.8)	66.2† (65.9–68.0)
Hemodynamics				
CO (L/min)	2.5 (2.2–3.2)	2.0* (2.0–3.0)	2.8 (2.7–3.3)	3.3† (3.2–3.9)
HF (/min)	72 (72–76)	67 (57–79)	86 (79–103)	96†‡ (91–113)
MAP (mm Hg)	77 (69–90)	69 (69–74)	76† (71–83)	69 (68–76)
MPAP (mm Hg)	22 (16–23)	30* (28–32)	30 (29–35)	35 (30–36)
CVP (mm Hg)	10 (7–12)	10 (10–11)	8 (7–10)	7 (7–8)
PCWP (mm Hg)	13 (12–14)	15 (13–16)	12 (11–14)	12 (8–12)
PVR ($dyn \cdot s \cdot cm^{-5}$)	260.5 (125.8–288)	627.5* (333.3–800.0)	407.2 (388.1–690.6)	509.1 (456.0–573.3)
SVR ($dyn \cdot s \cdot cm^{-5}$)	1994.2 (1711.6–2414.4)	1594.6 (1547.6–2313.7)	1628.7 (1552.2–2303.0)	1285.0† (1236.4–1719.9)
Oxygen transport and consumption				
$\dot{D}O_2$ (mL/min)	356.8 (281.6–391.4)	274.4* (237.3–287.3)	419.0† (326.9–465.1)	450.6† (381.1–468.5)
$\dot{V}O_2$ (mL/min)	105.3 (86.4–138.2)	135.6 (106.7–142.7)	153.4 (124.5–158.5)	104.0 (99.7–107.7)

Values provided as median (interquartile ranges).

PSV = pressure support ventilation; BIPAP + SB = biphasic positive airway pressure + spontaneous breathing; Pao_2/Fio_2 = ratio between arterial pressure of oxygen and inspired oxygen fraction; $\dot{Q}_{VA}/\dot{Q}_t$ = venous admixture; $Paco_2$ = arterial pressure of carbon dioxide; CO = cardiac output; HF = heart frequency; MAP = mean arterial blood pressure; MPAP = mean pulmonary arterial pressure; CVP = central venous pressure; PCWP = pulmonary artery wedge pressure; PVR = pulmonary vascular resistance; SVR = systemic vascular resistance; $\dot{D}O_2$ = oxygen delivery; $\dot{V}O_2$ = oxygen consumption.

* $P < 0.05$ versus baseline; † $P < 0.05$ versus injury; ‡ $P < 0.05$ versus PSV.

Table 3. Computed Tomography Data

	Controlled ventilation (square inspiratory flow pattern)		Assisted ventilation (decelerating inspiratory flow pattern)	
	Baseline	Injury	PSV	BIPAP + SB
Total lung volume (mL)	1015.1 (809.8–1161.9)	1025.9* (947.2–1295.5)	797.7† (706.6–974.1)	832.2† (825.1–948.2)
Total gas volume (mL)	718.4 (518.9–800.5)	621.0 (524.7–753.2)	320.5† (237.0–324.4)	310.7† (290.7–436.0)
Total lung mass (g)	296.7 (290.9–361.5)	495.5* (422.4–542.3)	560.7 (382.2–566.9)	522.8 (389.1–541.5)
Hyperinflated (% Vol)	3.0 (1.4–3.5)	2.3 (1.7–3.1)	0.9 (0.5–2.4)	0.9 (0.8–2.1)
Normally aerated (% Vol)	81.9 (77.0–83.1)	63.3* (61.2–69.0)	42.4† (33.0–49.0)	43.5† (34.9–54.6)
Poorly aerated (% Vol)	11.5 (10.8–14.0)	20.0 (17.5–22.8)	29.5 (24.3–29.8)	24.6 (20.2–26.1)
Nonaerated (% Vol)	2.6 (2.4–3.3)	11.5* (10.4–14.6)	32.7† (25.2–34.6)	28.7† (25.3–29.9)

Values provided as median (interquartile ranges). Hyperaerated, normally aerated, poorly aerated, and nonaerated compartments were computed according to references.[21,22]

PSV = pressure support ventilation; BIPAP + SB = biphasic positive airway pressure + spontaneous breathing.

* $P < 0.05$ versus baseline; † $P < 0.05$ versus injury; ‡ $P < 0.05$ versus PSV.

total lung mass, and volume of nonaerated areas were observed (Table 3).

As shown in Table 1, total minute ventilation increased with both modes of assisted mechanical ventilation ($P < 0.05$). The reduction of V_T during PSV and BIPAP + SB was accompanied by an increase in the total RR ($P < 0.05$). Additionally, a significant reduction of total gas volume and the volume of normally aerated areas were observed ($P < 0.05$, Table 3). Despite this, oxygenation increased and venous admixture decreased with both modes of assisted compared with controlled mechanical ventilation ($P < 0.05$), whereas $P_{0.1}$ and PTP were higher during BIPAP + SB than PSV. No significant differences between PSV and BIPAP + SB were observed with regard to gas exchange and distribution of aeration (Table 3).

Regional Distribution of Aeration and PBF

Figure 2 shows the three-dimensional representation of the distribution of lung aeration and PBF for one representative animal. At baseline, nonaerated areas were constrained to the most caudal regions. After induction of ALI, nonaerated areas increased in the dorsal lung zones, whereas normally aerated areas could be observed mainly in ventral and cranial regions. During PSV and BIPAP + SB, the amount of nonaerated areas in dorsal parts of the lungs increased further (Figs. 2 and 3A, left panels). Similarly, after ALI, PBF shifted from caudal and dorsal to cranial and ventral lung regions, respectively ($P < 0.05$). During PSV and BIPAP + SB, PBF further decreased in dorsal and caudal areas, but no differences were observed between modes (Figs. 2 and 3A, right panels).

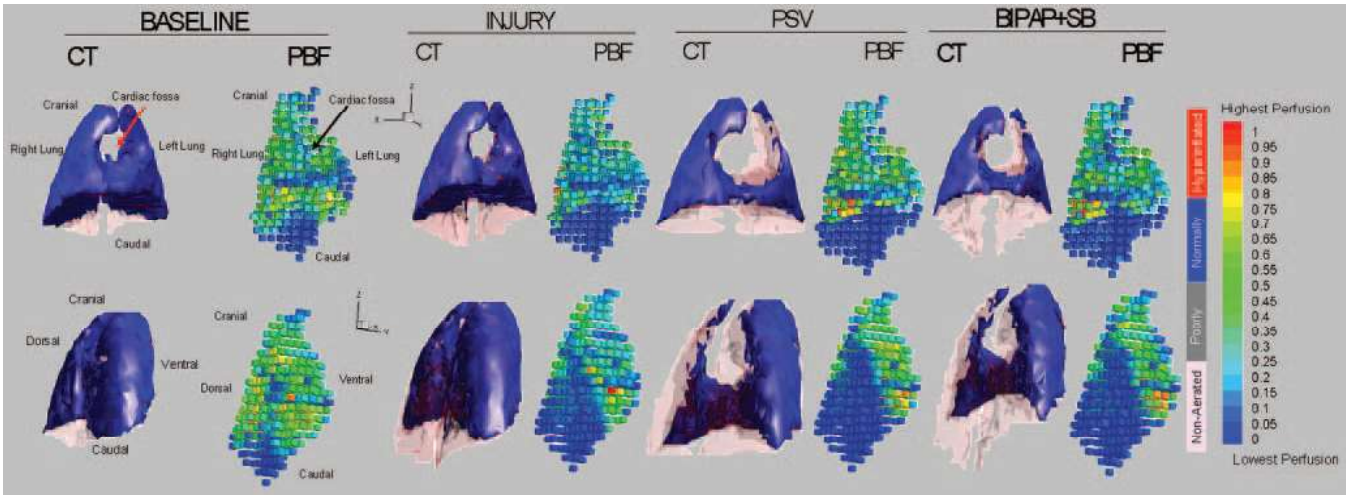

Figure 2. Three-dimensional representation of the distribution of aeration assessed by static computed tomography (CT), and the spatial distribution of weight-normalized relative pulmonary blood flow (PBF) in one representative animal. CT images were obtained at the end of expiration. The *x*, *y*, and *z* axes represent the spatial orientation of lungs. Two different projections are shown: the upper row presents a frontal plan projection and the lower row presents the same lungs rotated by 120° around the vertical axis (*z*). Red represents hyperaerated (−1000 to −900 Hounsfield units [HU]); blue, normally aerated (−900 to −500 HU); gray, poorly aerated (−500 to −100 HU); and pink, nonaerated areas (−100 to +100 HU). Color mapping was used to illustrate PBF, with the color intensity normalized by the maximum PBF at each experimental condition. The normalized color bar is presented with dark blue and red, representing the lowest and highest perfusion levels, respectively. Note the increase of poorly and nonaerated areas from the caudal to cranial and dorsal to ventral areas after induction of acute lung injury, as well as during assisted spontaneous breathing with pressure support ventilation (PSV) and with biphasic positive airway pressure and spontaneous breathing (BIPAP + SB). Also note the redistribution of PBF toward better aerated cranial and ventral lung regions.

Cluster Analysis

Figure 4 shows the results of the cluster analysis for the same animal. Lung pieces could be grouped into six main clusters in that animal (Fig. 4A, left panels). Cluster A presented an almost constant distribution of PBF. Cluster B presented a pattern of increase of PBF through all experimental interventions, whereas Cluster C presented the opposite pattern. Cluster D presented a decrease of PBF from controlled to assisted ventilation with PSV and BIPAP + SB, whereas Cluster F presented the opposite pattern. Cluster E presented a pattern of increase of PBF from baseline to injury, with a decrease of PBF from injury to PSV and BIPAP + SB.

The spatial distribution of clusters (Fig. 4A, right panel) evidenced a reduction of PBF in caudal and dorsal regions between baseline and injury (Cluster C), with a concomitant increase in the cranial and ventral regions (Clusters B and E). During PSV and BIPAP + SB, a further reduction of PBF in caudal and dorsal regions was observed (Clusters C, D, and E), as well as an increase in PBF to cranial and ventral regions (Clusters B and F).

Figure 4B shows the six clusters of the meta-cluster analysis (Fig. 4B, left panel). Cluster A presented an almost constant pattern of PBF under all experimental conditions. Cluster B presented an increase of PBF after SB was resumed, whereas Cluster F presented the opposite pattern. Cluster C presented a decrease of PBF throughout the experimental conditions, whereas Cluster D presented the reverse pattern. Cluster F presented an increase of PBF from baseline to injury and a decrease of PBF from controlled ventilation to SB. Figure 4B (middle panels) shows the percentages of the number of pieces of each animal related to the total amount of pieces of the meta-lung. Note that the clustering process was quite representative of the overall behavior. Figure 4B (right panels) shows the spatial distribution of meta-clusters. As can be observed, the clusters that presented a reduction in PBF were located in dorsal and caudal regions, whereas the clusters that presented an increase in PBF were located in ventral and cranial regions of lungs.

DISCUSSION

The main findings of this study were that: 1) in a surfactant depletion model of ALI, PSV and BIPAP + SB led to similar improvement in oxygenation and reduction in venous admixture compared with controlled mechanical ventilation; 2) $P_{0.1}$ and PTP were higher with BIPAP + SB than with PSV; 3) neither PSV nor BIPAP + SB resulted in increased aeration of dependent lung regions compared with controlled mechanical ventilation; 4) during PSV and BIPAP + SB, pulmonary perfusion shifted from dependent to nondependent lung regions.

Regional Distribution of Aeration and PBF During Controlled Mechanical Ventilation

Controlled mechanical ventilation with muscle paralysis modifies the displacement pattern of the diaphragm.[8,9] Accordingly, normally aerated and hyperaerated areas are usually located in nondependent regions, whereas poorly aerated and nonaerated areas

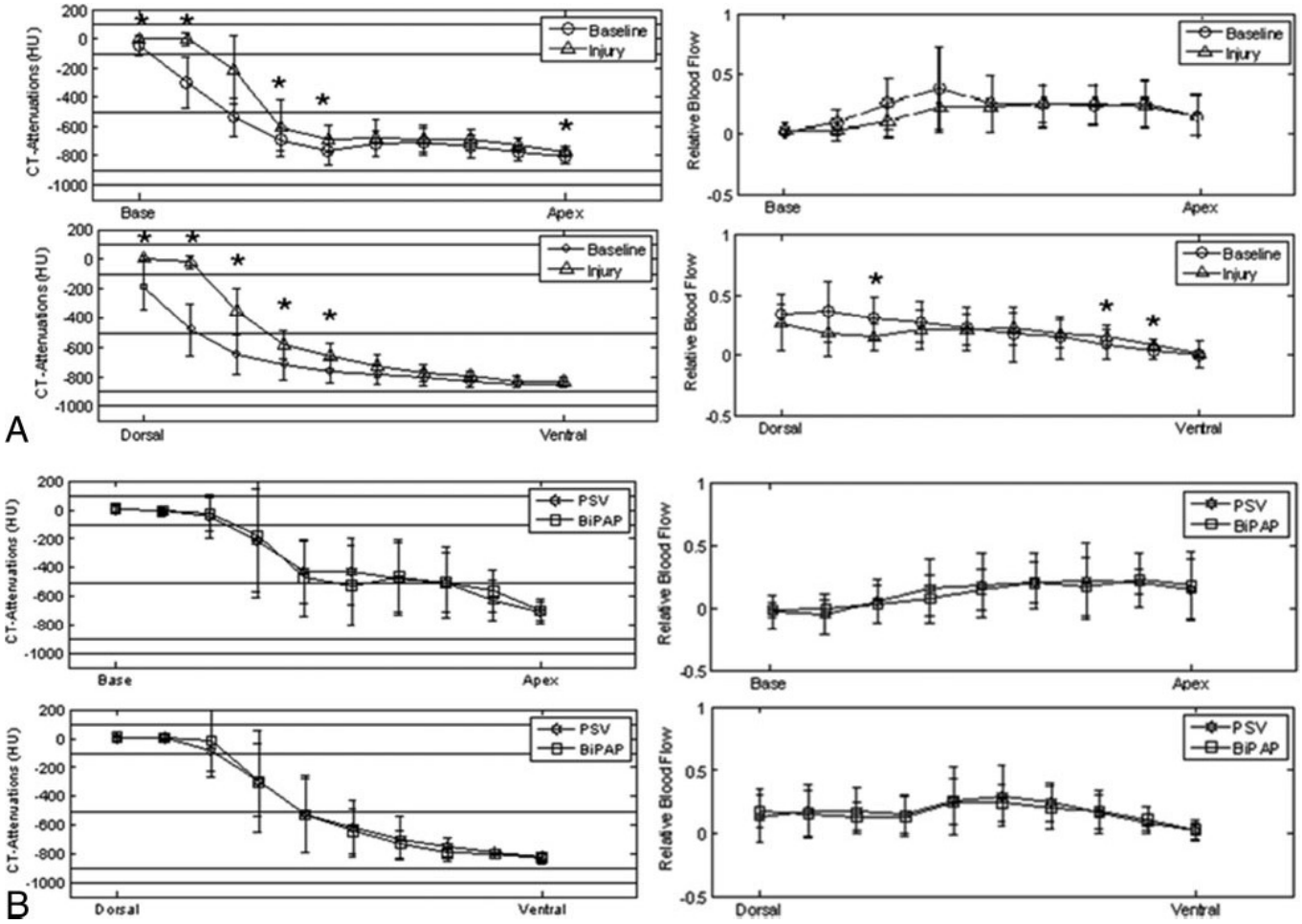

Figure 3. Left column: Regional distribution of computed tomography (CT) attenuation, expressed in Hounsfield units (HU), in 10 zones of lungs along the cranio-caudal (upper panels) and ventro-dorsal (lower panels) axes at Baseline and Injury (A) as well as at institution of pressure support ventilation (PSV) and biphasic positive airway pressure (BIPAP), respectively (B). The horizontal lines marked the ranges for each compartment in the CT attenuation plot. Symbols represent the median at each measurement condition, with circles, triangles, stars, and squares representing Baseline, Injury, assisted ventilation with PSV, and assisted ventilation with BIPAP, respectively. Right column: Regional distribution of the weight-normalized relative pulmonary blood flow content (PBF) in 10 zones along the cranio-caudal (upper panels) and ventro-dorsal (lower panels) axes. Vertical bars represent 1st and 3rd quartiles. *$P < 0.05$, Baseline versus Injury (controlled ventilation).

are seen in dependent lung regions.[10] Our results are in agreement with these observations.

The meta-cluster analysis showed a consistent pattern of changes in regional distribution of PBF across animals. Although PBF decreased in dorsal regions, an increase of blood flow in ventral regions occurred. However, no differences in the regional distribution of PBF were observed in more central parts of the lungs after induction of ALI, even though these regions presented large amounts of poorly or nonaerated lung tissue. The reduced but still present blood flow through the dorsal and caudal regions likely explains the increased venous admixture and the reduced Pao_2/Fio_2 ratio under controlled ventilation after induction of ALI.

Regional Distribution of Aeration and PBF During PSV and BIPAP + SB

SB activity has been proposed as an alternative to improve respiratory function and reduce sedation and circulatory drug support during ALI.[3] Although it cannot be considered a "gold standard," PSV is the most frequently used form of assisted mechanical ventilation in the clinical setting.[26] During PSV, every flow- or pressure-triggered breath is assisted with positive pressure, helping to unload the respiratory muscles and to reduce the work of breathing, as well as to enhance the synchrony between subject and mechanical ventilator. However, depending on the settings of the mechanical ventilator, excessive unloading of respiratory muscles can also lead to loss of movement of the diaphragm, especially in the posterior muscular sections, which would reduce the transpulmonary pressure in dependent lung regions and mimic-controlled ventilation.[5,8,11]

On the other hand, BIPAP + SB supports inspiration only if it begins simultaneously with the change from $CPAP_{low}$ to $CPAP_{high}$, but nonsupported breathing is possible in both levels. Although nonsupported breaths are associated with increased work of breathing, they may be useful to improve ventilation of

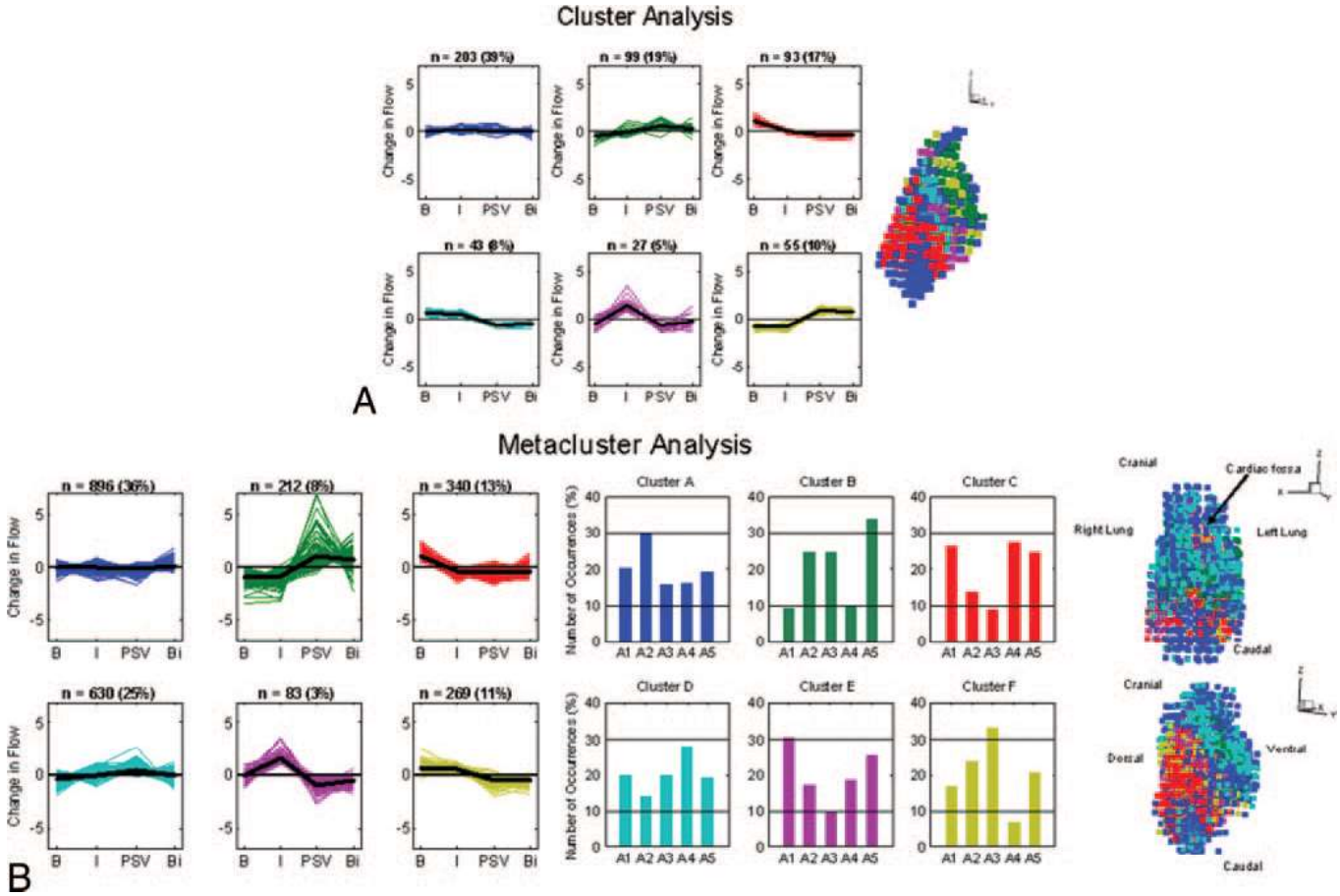

Figure 4. A, Patterns of changes in the residuals of the weight-normalized pulmonary blood flow of the pig presented in Figure 1, at each experimental intervention (B = baseline; I = injury; PSV = pressure support ventilation; Bi = biphasic positive airway pressure, left panels). Changes in flow for a piece at each specified experimental condition was calculated as the difference between the $\dot{Q}_{rel}$ at that condition and the mean $\dot{Q}_{rel}$ throughout all experimental interventions. Six patterns of changes in pulmonary blood flow (clusters) were identified by the nonhierarchical analysis. Each cluster is depicted with different colors (left panels, Clusters A–F). The number of pieces in each cluster and the percentage of each cluster in the total lung are also exhibited above each panel. Right: Three-dimensional representation of the spatial distribution of the six color-coded clusters. B, Clusters identified through the nonhierarchical clustering method throughout all experimental conditions in all animals (meta-cluster analysis). The number of pieces in each cluster and the percentage of each cluster in the total meta-lung are also exhibited above each panel. The bold lines represent the mean value of the respective color-coded cluster. Middle panels: Percentage (number of occurrences) of pieces from each animal (A1–A5) in the respective clusters; horizontal lines mark the range of 20% ± 10%. Right: Three-dimensional representation of the spatial distribution of the six color-coded clusters (meta-lung). Two different projections are shown. The upper right panel presents a frontal plan projection and the lower right panel presents the same picture rotated by 120° along the vertical axis (*z*). The *x*, *y*, and *z* axes represent the spatial orientation of the meta-lung.

dependent lung areas by means of contraction of the posterior muscular sections of the diaphragm and also increase lung perfusion through reduction of intrathoracic pressure. Accordingly, different authors have suggested that BIPAP + SB leads to an improvement in lung function when compared with PSV, as a consequence of the better matching of ventilation/perfusion ratio in dependent regions.[17,18] However, the distribution of PBF is influenced by different factors, such as gravity, the fractal structure of pulmonary capillaries, trans-capillary pressure gradients, and, most importantly, hypoxic pulmonary vasoconstriction.[27–30]

Our findings are in line with previous studies showing that PSV and BIPAP + SB improve oxygenation and reduce venous admixture compared with controlled ventilation.[16–18] Additionally, our results showed a significant increase in the respiratory drive and in PTP, which reflects the respiratory effort and the oxygen consumption of the respiratory muscles,[31] during BIPAP + SB compared with PSV. Thus, we expected that the respiratory muscles, and more particularly the diaphragm, would generate higher transpulmonary pressures in dependent zones during BIPAP + SB, resulting in recruitment and improved ventilation/perfusion matching in those zones. However, the improvement in pulmonary function could not be attributed to increased end-expiratory lung gas volumes or normally aerated areas. This result is somewhat surprising, given that the surfactant depletion model is believed to be a very recruitable model of ALI.[32,33] However, we cannot exclude the possibility that SB may have influenced the distribution of

regional ventilation or that intratidal lung recruitment occurred.

It is worth noting that the redistribution of intrapulmonary gas with PSV and BIPAP + SB was followed by the same pattern of the redistribution of PBF. Two clusters representing 33% of the total lung tissue and situated in ventral areas revealed an increase of PBF with PSV and BIPAP + SB. In contrast, two other clusters representing 14% of lung tissue and situated in dorsal areas showed a decrease of PBF. These findings support the hypothesis that improved regional aeration/perfusion matching occurred during assisted ventilation with PSV and BIPAP + SB. On the other hand, the regional distribution of aeration and PBF did not differ between PSV and BIPAP + SB, as we expected. The most likely explanation for redistribution of PBF toward nondependent lung regions is that peak and mean Paw were lower during PSV and BIPAP + SB than during controlled mechanical ventilation. Thus, lung capillaries in nondependent lung zones probably had lower impedance to perfusion, allowing more efficient hypoxic pulmonary vasoconstriction in dependent areas. Because both PSV and BIPAP + SB used decelerating inspiratory flow, whereas controlled ventilation used square inspiratory flow, we also cannot exclude that redistribution of airway-alveolar flow improved ventilation in nondependent zones during assisted compared with controlled mechanical ventilation. In addition, it is possible that the rapid shallow breathing pattern and hypercapnia observed during assisted mechanical ventilation further contributed to a shift of ventilation to nondependent zones.

In contrast to our study, other authors have reported increased oxygenation and reduced venous admixture with BIPAP + SB compared with PSV.[17] This is possibly explained by the fact that those authors did not match assisted ventilation modes for both mean Paw and minute ventilation simultaneously, as performed in this work. Our findings also differ from the clinical reports by Cereda et al.[34] and Putensen et al.[17] One possible explanation is that patients investigated in those studies may have presented more severe lung injury. Another possible reason is that patients with ALI/acute respiratory distress syndrome may exhibit blunted hypoxic pulmonary vasoconstriction[35] because of the inhibitory effects of proinflammatory mediators, nitric oxide, and endotoxin itself.[36–39]

Possible Clinical Implications

Our findings contribute to further understand the physiological mechanisms leading to improvement of Pao_2 and reduction of venous admixture when switching from controlled to assisted spontaneous mechanical ventilation. According to our data, redistribution of PBF from dependent toward nondependent, better aerated regions, which is closely related to preserved hypoxic pulmonary vasoconstriction, may play a pivotal role in improvement of oxygenation during assisted mechanical ventilation. Consequently, lack of improvement of Pao_2 after resuming SB in mechanically ventilated patients may suggest impairment of hypoxic pulmonary vasoconstriction and/or diffuse loss of lung aeration.

Limitations

This study has several limitations. First, we used a relatively low positive end-expiratory pressure level (5 cm H_2O), which possibly precluded the more dependent alveolar units from being kept open at the end of expiration, even if they may have opened during inspiration (intratidal recruitment). Second, we did not use a crossover design for controlled and assisted ventilation, which may have somewhat biased our analysis. We decided for the fixed sequence of controlled followed by assisted mechanical ventilation because it more closely reflects clinical practice. Moreover, if we had included controlled ventilation in the randomization, redistribution of PBF during PSV and BIPAP + SB could have "contaminated" controlled ventilation (carryover effect). Third, we evaluated only immediate physiological effects of PSV and BIPAP + SB. Thus, we cannot exclude that these modes may lead to recruitment of dependent lung zones over the long term. Fourth, depth of sedation was increased during controlled compared with assisted mechanical ventilation. However, the drugs we used, namely midazolam, ketamine and remifentanil, seem not to influence the tonus of pulmonary vasculature.[40,41] Fifth, it must be kept in mind that our evaluation was performed in a model of ALI that does not reproduce all features of the more complex human ALI/acute respiratory distress syndrome. Because PSV and BIPAP + SB seem to be more likely to result in improved lung function when the hypoxic vasoconstriction reflex is preserved, extrapolation of our results to the clinical scenario must consider this fact.

We conclude that in a surfactant depletion model of ALI, PSV and BIPAP + SB improve oxygenation and reduce venous admixture to similar extents compared with controlled ventilation. Such effects are better explained by redistribution of lung perfusion toward nondependent lung zones than recruitment of dependent lung regions.

REFERENCES

1. Hering R, Zinserling J, Wrigge H, Varelmann D, Berg A, Kreyer S, Putensen C. Effects of spontaneous breathing during airway pressure release ventilation on respiratory work and muscle blood flow in experimental lung injury. Chest 2005;128:2991–8
2. Putensen C, Hering R, Muders T, Wrigge H. Assisted breathing is better in acute respiratory failure. Curr Opin Crit Care 2005;11:63–8
3. Putensen C, Muders T, Varelmann D, Wrigge H. The impact of spontaneous breathing during mechanical ventilation. Curr Opin Crit Care 2006;12:13–8

4. Putensen C, Zech S, Wrigge H, Zinserling J, Stuber F, Von ST, Mutz N. Long-term effects of spontaneous breathing during ventilatory support in patients with acute lung injury. Am J Respir Crit Care Med 2001;164:43–9
5. Putensen C, Hering R, Wrigge H. Controlled versus assisted mechanical ventilation. Curr Opin Crit Care 2002;8:51–7
6. Wrigge H, Zinserling J, Neumann P, Defosse J, Magnusson A, Putensen C, Hedenstierna G. Spontaneous breathing improves lung aeration in oleic acid-induced lung injury. Anesthesiology 2003;99:376–84
7. Levine S, Nguyen T, Taylor N, Friscia ME, Budak MT, Rothenberg P, Zhu J, Sachdeva R, Sonnad S, Kaiser LR, Rubinstein NA, Powers SK, Shrager JB. Rapid disuse atrophy of diaphragm fibers in mechanically ventilated humans. N Engl J Med 2008;358:1327–35
8. Froese AB, Bryan AC. Effects of anesthesia and paralysis on diaphragmatic mechanics in man. Anesthesiology 1974;41:242–55
9. Froese AB. Anesthesia-paralysis and the diaphragm: in pursuit of an elusive muscle. Anesthesiology 1989;70:887–90
10. Puybasset L, Cluzel P, Gusman P, Grenier P, Preteux F, Rouby JJ. Regional distribution of gas and tissue in acute respiratory distress syndrome. I. Consequences for lung morphology. CT Scan ARDS Study Group. Intensive Care Med 2000;26:857–69
11. Duggan M, Kavanagh BP. Pulmonary atelectasis: a pathogenic perioperative entity. Anesthesiology 2005;102:838–54
12. Wrigge H, Zinserling J, Neumann P, Muders T, Magnusson A, Putensen C, Hedenstierna G. Spontaneous breathing with airway pressure release ventilation favors ventilation in dependent lung regions and counters cyclic alveolar collapse in oleic-acid-induced lung injury: a randomized controlled computed tomography trial. Crit Care 2005;9:R780–9
13. Putensen C, von ST, Hering R, Stuber F, Zinserling J. Effect of different ventilatory support modalities on the ventilation to perfusion distributions. Acta Anaesthesiol Scand Suppl 1997; 111:119–22
14. Hering R, Viehofer A, Zinserling J, Wrigge H, Kreyer S, Berg A, Minor T, Putensen C. Effects of spontaneous breathing during airway pressure release ventilation on intestinal blood flow in experimental lung injury. Anesthesiology 2003;99:1137–44
15. Varelmann D, Wrigge H, Zinserling J, Muders T, Hering R, Putensen C. Proportional assist versus pressure support ventilation in patients with acute respiratory failure: cardiorespiratory responses to artificially increased ventilatory demand. Crit Care Med 2005;33:1968–75
16. Gama de Abreu M, Spieth PM, Pelosi P, Carvalho AR, Walter C, Schreiber-Ferstl A, Aikele P, Neykova B, Hubler M, Koch T. Noisy pressure support ventilation: a pilot study on a new assisted ventilation mode in experimental lung injury. Crit Care Med 2008;36:818–27
17. Putensen C, Mutz NJ, Putensen-Himmer G, Zinserling J. Spontaneous breathing during ventilatory support improves ventilation-perfusion distributions in patients with acute respiratory distress syndrome. Am J Respir Crit Care Med 1999;159:1241–8
18. Henzler D, Pelosi P, Bensberg R, Dembinski R, Quintel M, Pielen V, Rossaint R, Kuhlen R. Effects of partial ventilatory support modalities on respiratory function in severe hypoxemic lung injury. Crit Care Med 2006;34:1738–45
19. Gama de Abreu M, Quelhas AD, Spieth P, Brauer G, Knels L, Kasper M, Pino AV, Bleyl JU, Hubler M, Bozza F, Salluh J, Kuhlisch E, Giannella-Neto A, Koch T. Comparative effects of vaporized perfluorohexane and partial liquid ventilation in oleic acid-induced lung injury. Anesthesiology 2006;104:278–89
20. Bleyl JU, Ragaller M, Tscho U, Regner M, Kanzow M, Hubler M, Rasche S, Albrecht M. Vaporized perfluorocarbon improves oxygenation and pulmonary function in an ovine model of acute respiratory distress syndrome. Anesthesiology 1999;91:461–9
21. Vieira SR, Puybasset L, Richecoeur J, Lu Q, Cluzel P, Gusman PB, Coriat P, Rouby JJ. A lung computed tomographic assessment of positive end-expiratory pressure-induced lung overdistension. Am J Respir Crit Care Med 1998;158:1571–7
22. Gattinoni L, Caironi P, Pelosi P, Goodman LR. What has computed tomography taught us about the acute respiratory distress syndrome? Am J Respir Crit Care Med 2001;164:1701–11
23. Hubler M, Souders JE, Shade ED, Polissar NL, Schimmel C, Hlastala MP. Effects of vaporized perfluorocarbon on pulmonary blood flow and ventilation/perfusion distribution in a model of acute respiratory distress syndrome. Anesthesiology 2001;95:1414–21
24. Lachmann B, Robertson B, Vogel J. In vivo lung lavage as an experimental model of the respiratory distress syndrome. Acta Anaesthesiol Scand 1980;24:231–6
25. Hlastala MP, Lamm WJ, Karp A, Polissar NL, Starr IR, Glenny RW. Spatial distribution of hypoxic pulmonary vasoconstriction in the supine pig. J Appl Physiol 2004;96:1589–99
26. Esteban A, Ferguson ND, Meade MO, Frutos-Vivar F, Apezteguia C, Brochard L, Raymondos K, Nin N, Hurtado J, Tomicic V, Gonzalez M, Elizalde J, Nightingale P, Abroug F, Pelosi P, Arabi Y, Moreno R, Jibaja M, D'Empaire G, Sandi F, Matamis D, Montanez AM, Anzueto A. Evolution of mechanical ventilation in response to clinical research. Am J Respir Crit Care Med 2008;177:170–7
27. Glenny RW, Robertson HT. Fractal modeling of pulmonary blood flow heterogeneity. J Appl Physiol 1994;70:1024–30
28. Glenny RW, Lamm WJ, Bernard SL, An D, Chornuk M, Pool SL, Wagner WW Jr, Hlastala MP, Robertson HT. Selected contribution: redistribution of pulmonary perfusion during weightlessness and increased gravity. J Appl Physiol 2000;89:1239–48
29. Altemeier WA, McKinney S, Glenny RW. Fractal nature of regional ventilation distribution. J Appl Physiol 2000;88:1551–7
30. Starr IR, Lamm WJ, Neradilek B, Polissar N, Glenny RW, Hlastala MP. Regional hypoxic pulmonary vasoconstriction in prone pigs. J Appl Physiol 2005;99:363–70
31. McGregor M, Becklake MR. The relationship of oxygen cost of breathing to respiratory mechanical work and respiratory force. J Clin Invest 1961;40:971–80
32. Van der Kloot TE, Blanch L, Youngblood AM, Weinert C, Adams AB, Marini JJ, Shapiro RS, Nahum A. Recruitment maneuvers in three experimental models of acute lung injury. Effect on lung volume and gas exchange. Am J Respir Crit Care Med 2000;161:1485–94
33. Luecke T, Meinhardt JP, Herrmann P, Weiss A, Quintel M, Pelosi P. Oleic acid vs saline solution lung lavage-induced acute lung injury: effects on lung morphology, pressure-volume relationships, and response to positive end-expiratory pressure. Chest 2006;130:392–401
34. Cereda M, Foti G, Marcora B, Gili M, Giacomini M, Sparacino ME, Pesenti A. Pressure support ventilation in patients with acute lung injury. Crit Care Med 2000;28:1269–75
35. Schuster DP, Anderson C, Kozlowski J, Lange N. Regional pulmonary perfusion in patients with acute pulmonary edema. J Nucl Med 2002;43:863–70
36. Schuster DP, Haller J. Regional pulmonary blood flow during acute pulmonary edema: a PET study. J Appl Physiol 1990; 69:353–61
37. Spohr F, Cornelissen AJ, Busch C, Gebhard MM, Motsch J, Martin EO, Weimann J. Role of endogenous nitric oxide in endotoxin-induced alteration of hypoxic pulmonary vasoconstriction in mice. Am J Physiol Heart Circ Physiol 2005;289:H823–31
38. Ichinose F, Zapol WM, Sapirstein A, Ullrich R, Tager AM, Coggins K, Jones R, Bloch KD. Attenuation of hypoxic pulmonary vasoconstriction by endotoxemia requires 5-lipoxygenase in mice. Circ Res 2001;88:832–8
39. Caironi P, Ichinose F, Liu R, Jones RC, Bloch KD, Zapol WM. 5-Lipoxygenase deficiency prevents respiratory failure during ventilator-induced lung injury. Am J Respir Crit Care Med 2005;172:334–43
40. Nakayama M, Murray PA. Ketamine preserves and propofol potentiates hypoxic pulmonary vasoconstriction compared with the conscious state in chronically instrumented dogs. Anesthesiology 1999;91:760–71
41. Bjertnaes L, Hauge A, Kriz M. Hypoxia-induced pulmonary vasoconstriction: effects of fentanyl following different routes of administration. Acta Anaesthesiol Scand 1980;24:53–7